Journal of the Civil Engineering Forum, May 2024, 10(2):123-132
DOI 10.22146/jcef.9151
Available Online at https://jurnal.ugm.ac.id/v3/jcef/issue/archive

Structural Health Assessment of Kretek II Bridge using Enhanced Frequency Domain Decomposition

Didib Astalis Ulul Absor*, Akhmad Aminullah, Bambang Supriyadi
Department of Civil and Environmental Engineering, Universitas Gadjah Mada, Yogyakarta, INDONESIA
Jalan Grafika No 2 Yogyakarta
*Corresponding author: didibastalis2017@mail.ugm.ac.id

SUBMITTED 24 August 2023 **REVISED** 19 January 2024 **ACCEPTED** 12 February 2024

ABSTRACT The development of infrastructure is growing rapidly in Indonesia. Kretek II bridge is one of the infrastructures built in the country. Dynamics aspects are one of the very important aspects used to validate structural analysis model or being linked to Structural Health Monitoring (SHM) of the bridge. Dynamics properties such as natural frequency, damping ratio, and mode shape also referred as modal parameters. The objective of this research is to determine the modal parameters of Kretek II bridge using Enhanced Frequency Domain Decomposition (EFDD) which is commonly used to extract modal parameters from the acceleration data recorded. Compared to the conventional method, EFDD is very practical and robust in structural health assessment because of its user-friendly uses in the ARTeMIS Modal software. To make sure that the results from EFDD are accurate, numerical modeling is necessary to validate it. This research was conducted using dynamics load test results as data for the modal extraction with EFDD method assisted by ARTeMIS Modal software. Dynamics load test was performed by placing 8 accelerometers in the span and exciting it with impact load from dropped truck on ramp. Modal parameters from the EFDD results are then compared to the numerical modeling results. The first two modes of the EFDD and numerical modeling results consecutively are 3.09 Hz, 3.745 Hz and 3.06 Hz, 3.49 Hz. The EFDD and numerical modeling results are both in agreement with both results having similar mode shape on their first two mode and low error percentage with only 0.89% and 7.17% respectively.

KEYWORDS Modal Analysis; Dynamics Load Test; Structural Health Monitoring; EFDD; ARTeMIS

1 INTRODUCTION

Indonesia's infrastructure has seen rapid expansion over the past decade. Numerous infrastructure construction projects are underway in various locations. Among them is the construction of the Kretek II bridge, which features a PCI Girder superstructure. The bridge spans the Kretek River, connecting Tirtohargo Village and Parangtritis.

Following the construction of the Kretek II bridge, a series of tests were conducted to ensure adherence to the design plan. The conducted tests include both static and dynamic load testing. The dynamic aspect is crucial from a structural perspective. It is commonly used for validating structural analysis model and closely linked to Structural Health Monitoring (SHM) (Brincker and Ventura, 2015). Understanding this dynamics aspect also helps to mitigate risks such as the amplification of deflection, stress, and strain due to resonant vibrations (Schwarz and Richardson, 1999). One method to detect damage or deterioration of a structure is by observing changes in the natural frequency (Salawu, 1997). Not only the natural frequency, but the damping ratio and mode shapes are also important parameters in this dynamic aspect, commonly referred to as modal parameters. Modal analysis is necessary to identify these parameters.

Experimental modal analysis (EMA) and operational modal analysis (OMA) are two commonly used methods to determine the modal parameters of a structure. EMA is deemed more reliable but less practical due to its requirement for undisturbed conditions and controlled excitation (Orlowitz and Brandt, 2017). This often leads to EMA being performed only when the bridge is temporarily closed or not in operation. In contrast, OMA can be performed under any conditions without the need for measuring excitation loads.

The Frequency Domain Decomposition (FDD) method is commonly used to extract modal parameters in modal analysis. This method decomposes multiple response systems into a series of Single Degree of Freedom (SDOF) responses for each mode. The modal parameters encompasses the natural frequency, mode shapes, and the damping ratio of the structure. During the initial stage of the development, FDD was limited to extract only natural frequencies and mode shapes. Methods to determine the damping ratio were later developed in the following year (Brincker and Zhang, 2009; Brincker et al., 2001, 2000*a*,*c*,*b*). This method can analyze various structures, including bridges, high-rise buildings, and even dams. It is one of the robust and efficient methods for extracting modal parameters

(Ghalishooyan et al., 2019; Zair et al., 2020; Sevim et al., 2010; Ma and Luan, 2020). This method also advances conventional frequency-domain estimation to analyze case with closely spaced modes (Brincker and Ventura, 2015). To ensure the accuracy of the obtained mode shapes, Modal Assurance Criterion (MAC) analysis is performed to assess the relationship and similarity between the generated modes (Pastor et al., 2012). Additional, finite element or numerical model are required as another means of validation for the modal analysis (Silva and Neves, 2020; El-Borgi et al., 2004; Mao et al., 2019).

The aim of this research is to determine the modal parameters of the Kretek II bridge using the Enhanced Frequency Domain Decomposition (EFDD) method, an advanced version of the FDD method. EFDD is highly practical and powerful in structural health assessment due to its user-friendly interface and implementation within the ARTeMIS Modal software, as compared to the conventional methods. This had made the EFDD method one of the preferred alternatives in structural health assessment for modal analysis. This research processes the experimental data obtained from the dynamics load test results to extract all the modal parameters, including natural frequency, mode shapes, and damping ratio. The extracted modal parameters are then compared to the numerical modeling to validate the results.

2 THEORETICAL BACKGROUND

To understand structural dynamics, it's crucial to recognize that the dynamics equation is affected by mass, stiffness, and damping (see Equation 1).

$$mx + cx + kx = F(t) \tag{1}$$

Where m is mass, c is damping, k is stiffness, while F(t) is external forces.

All these factors are linked to the material used in the structure, which is the main reason we can use them as indicators to assess the structural health and condition. Since these factors also used to determine the natural frequency of the structure, any changes in the natural frequency between two point in time will serve as a significant indicator to detect structural damage or deterioration.

EFDD is widely used to identify modes of the structure (Brincker and Zhang, 2009). This method is formulated based on the unknown inputs $x(t)$ and the measured responses $y(t)$ (see Equation 2).

$$G_y y(j) = H(j) G_x x(j) H(j)^T \tag{2}$$

where Gxx is $r \times r$ matrix of Power Spectral Density (PSD) from the inputs, r is the number of inputs, $G_{yy}(j\omega)$ is $m \times m$ matrix PSD from the responses, m is the number of responses, and $H(j\omega)$ is $m \times r$ matrix from FRF. This FRF can also be expressed in pole/residue form as a partial equation (see Equation 3)

$$H(j) = \sum_{k=1}^{n} \frac{R_k}{j - {}_k} + \frac{\bar{R}_k}{j - \bar{\lambda}_k} \tag{3}$$

with n is the number of modes, λ_k is the pole, while R_k is the residue. Thus, R_k is obtained by formulating mode shape vector and modal participation vector (see Equation 4).

$$R_k = \phi_k \gamma_k^T \tag{4}$$

where ϕ_k is the mode shape vector and γ_k is the modal participation vector. Assuming the inputs is a clear white noise, and its PSD is a constant matrix, Equation 1 can be expressed as Equation 5.

$$G_{yy}(j\omega) = \sum_{k=1}^{n} \sum_{s=1}^{n} \left[\frac{R_k}{j - {}_k} + \frac{\bar{R}_k}{j - \bar{\lambda}_k} \right] C \left[\frac{R_s}{j - {}_s} + \frac{\bar{R}_s}{j - \bar{\lambda}_s} \right]^H \tag{5}$$

where H is the transpose and complex conjugation. If both partial equations are multiplied using the Heaviside partial fraction theorem, the output PSD can be simplified in pole/residue form (see Equation 6).

$$G_{yy}(j\omega) = \sum_{k=1}^{n} \frac{A_k}{j - {}_k} + \frac{\bar{A}_k}{j - \bar{\lambda}_k} + \frac{B_k}{-j - {}_k} + \frac{\bar{B}_k}{-j - \bar{\lambda}_k} \tag{6}$$

where A_k is the k'th residue matrix from the output PSD (see Equation 7). The contribution to the residue from the k'th mode can also be simplified (see Equation 8). Assuming it has light damping, the residue becomes equivalent to the mode shape vector (see Equation 9).

$$A_k = R_k C \left(\sum_{s=1}^{n} \frac{\bar{R}_k^T}{-\lambda - \bar{\lambda}_s} + \frac{R_s^T}{-\lambda_k - \lambda_s} \right) \tag{7}$$

$$A_k = \frac{R_k C \bar{R}_k^T}{2\alpha_k} \tag{8}$$

$$A_k \propto R_k C \bar{R}_k = \phi_k \gamma_k^T C \gamma_k \phi_k^T = d_k \phi_k \phi_k^T \tag{9}$$

where α_k is minus real number of the pole with $\gamma_k = \alpha_k + j\omega_k$ and d_k is scalar constant. By denoting the limited number of modes at certain frequency γ with Sub(ω), the response spectral density can be expressed (see Equation 10).

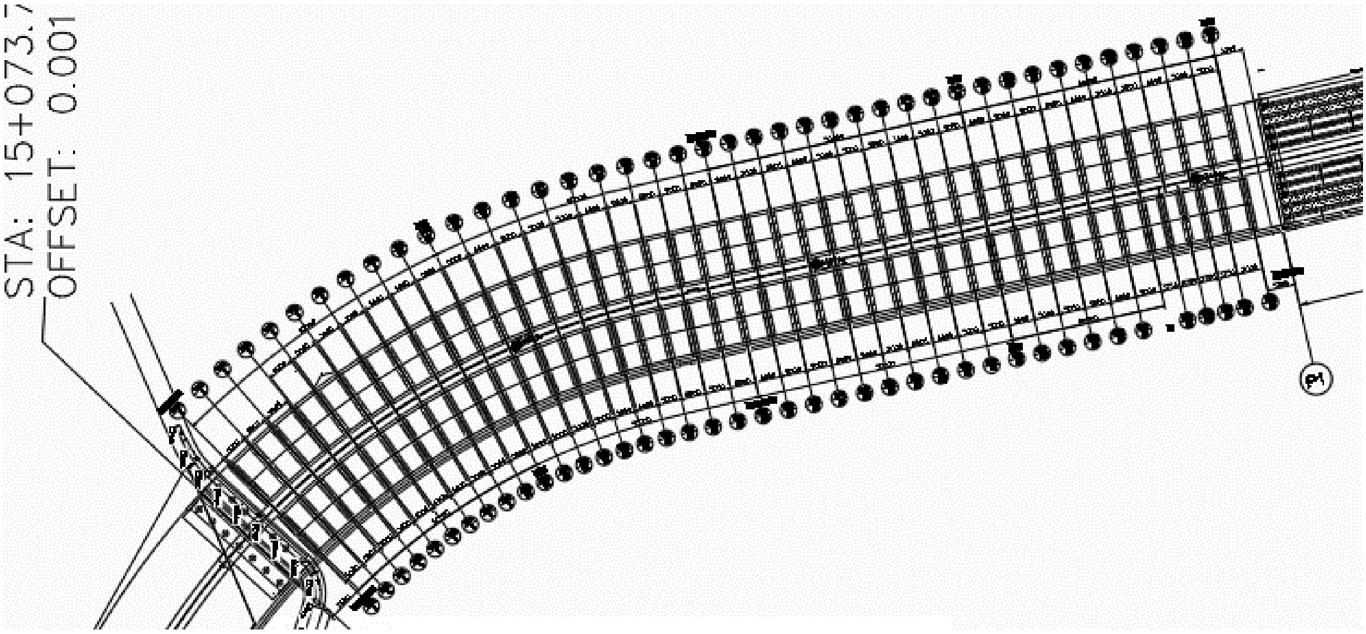

Figure 1 Slab on pile on Kretek II bridge

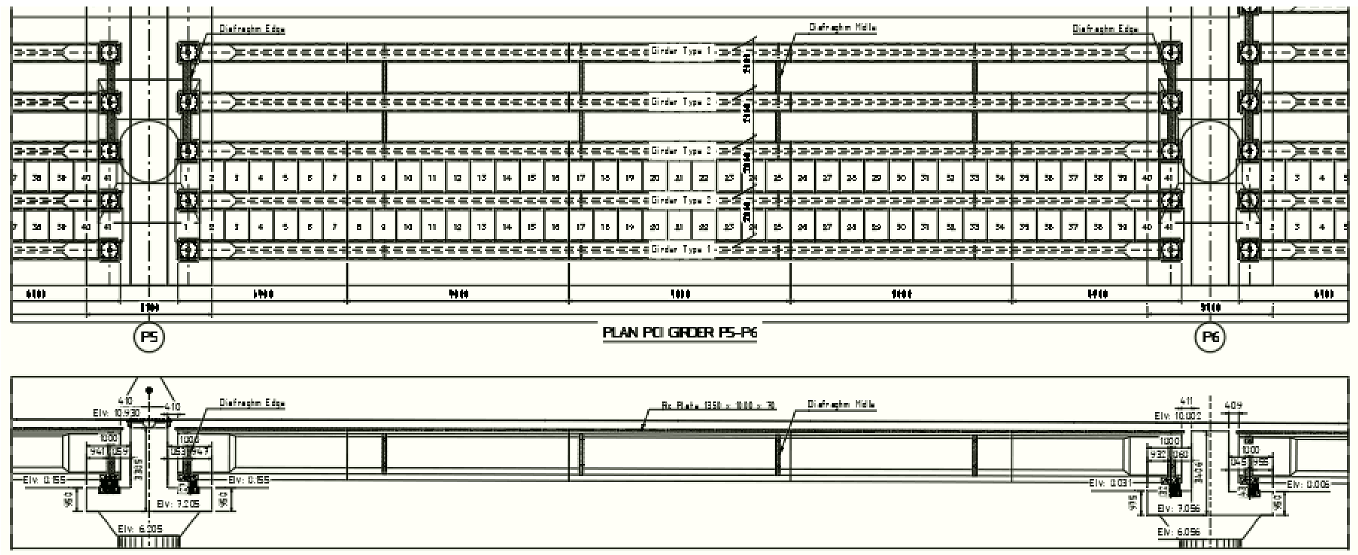

Figure 2 PCI Girder on P5-P6 Kretek II bridge

(a) Laptop (b) Triaxial accelerometer (c) Access point

Figure 3 Setup used in the dynamic load test

$$G_{yy}(j\omega) = \sum_{k=sub(\omega)} \frac{d_k \phi_k \phi_k^T}{j\omega - \lambda_k} + \frac{\bar{d}_k \bar{\phi}_k \bar{\phi}_k^T}{j\omega - \bar{\lambda}_k} \tag{10}$$

To use FDD, the output PSD matrix needs to be estimated and then decomposed by taking singular value decomposition (SVD) on it (see Equation 11).

$$G_{yy}(j\omega_i) = U_i S_i U_i^H \tag{11}$$

where U_i is the unitary matrix containing the singular vector u_{fj} while S_i is the diagonal matrix containing the singular value of s_{if}. This first singular value vector in the possible close mode is the estimation of the mode shape (see Equation 12). Therefore, the natural frequency and damping can be obtained.

$$\hat{\phi} = u_{i1} \tag{12}$$

3 RESEARCH METHODS

3.1 Kretek II Bridge

The kretek II Bridge, located in Kretek, Bantul, Special Region of Yogyakarta, Indonesia, spans 2015 m, connecting Tirtohargo Village and Parangtritis Village. Its superstructure comprises PCI Girders with a length of 43.12 m, consisting of 8 spans. The bridge measures 24.5 m in width, featuring a main lane width of 7 m. Additionally, the bridge includes a 20-meter-long Slab on Pile structure, with a 5-meter spacing between each pile, and an expansion joint every 50 m (see Figure 1). The structure continues with PCI girders spanning 40.8 m, consisting of 8 spans. The distance between pile axes is 43.12 m (see Figure 2).

3.2 Dynamic Load Test

Only one span was reviewed, namely P5-P6 span. Since all spans were identical, only one test was conducted on this span. The dynamic load test took place on September 24-25, 2022. Several tools required for conducting the dynamic load test are listed below (see Figure 3):

1. data logger,
2. laptop,
3. power supply/battery,
4. triaxial accelerometer, and
5. access point/wireless repeater.

Eight accelerometers were deployed for the testing. Two were positioned on each side of the span at ¼, ½, and ¾ points along the span, with an additional one at each end of the supports. However, only 6 accelerometers were used for data collection, excluding those at supports' end (see Figure 4). Accelerometers are crucial tools for recording and monitoring acceleration data. Besides acceleration, they can also capture deflection and velocity by further integrating the acceleration data. Thus, accelerometer are widely used for measuring vibration (Morris and Langari, 2012).

The excitation load for this dynamic load test was provided by the impact load from a truck, making it considered as an EMA (Experimental Modal Analysis) (Schwarz and Richardson, 1999; Brincker and Ventura, 2015). During the test, an impact load from an empty truck was applied. The rear wheels of the truck were positioned in the middle of the span and dropped by pushing the truck from a 20 cm high ramp (see Figure 5).

Modal parameters were extracted from the bridge using the Enhanced Frequency Domain Decomposition (EFDD) method, assisted by ARTeMIS Modal software, and further validated with numerical modeling using Midas Civi. The dynamics load test results, obtained data from each accelerometer used in the testing (excluding those at the end of each support), are presented in Figure 6. It is evident from Figure 6 that the acceleration fluctuates at a specific point when the impact load of truck has been applied. This data will be utilized later as input data for ARTeMIS Modal. To closely and clearly observe the dynamics response from the impact load of truck, data cutting and filtering were required. The data recorded from accelerometers were filtered with a low-pass filter (see Figure 7).

3.3 Modeling concept

As previously mentioned, this paper focuses solely on the span between P5-P6. The total length of this span is typically 40.8 m, using PCI Girder with a standard manufactured profile of 2.1 m. The span comprises 5 girders, spaced 2 m apart, and is divided into 5 segments with 6 diaphragms separating them (see Figure 8). This configuration will serve as the foundation for numerical modeling later.

4 RESULTS

4.1 Enhanced Frequency Domain Decomposition (EFDD)

Table 1. Results from EFDD in ARTeMIS Modal

Mode No	Frequency (Hz)	Damping (%)	Complexity (%)	Mode Type
1	3.09	3.431	0.705	Vertical bending
2	3.745	1.681	13.501	Torsion
3	16,122	0,845	18,848	Vertical bending

The Dynamic Load Test generated acceleration data recorded from accelerometer responses on each installed sensor (see Figure 6 and 7). These recorded

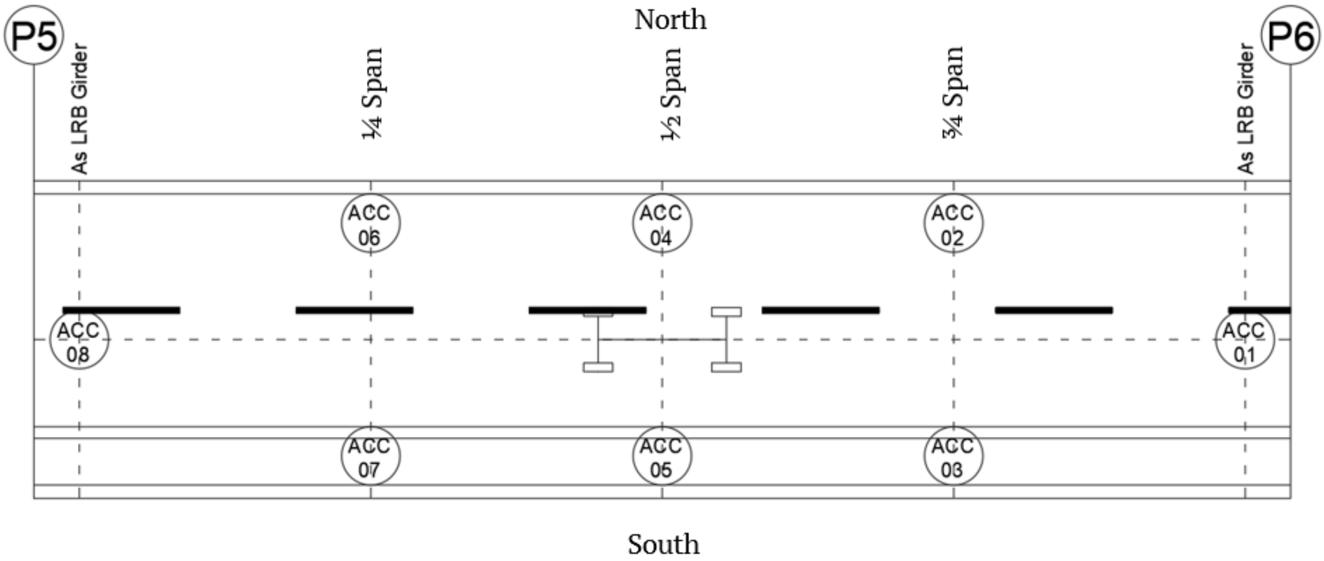

Figure 4 Accelerometer position sensor on P5-P6 Kretek II bridge

Figure 5 Impact load from truck as excitation load in dynamic load test

Table 2. Results of MAC Comparison

Mode	3.1 Hz	3.7 Hz	16.1 Hz
3.1 Hz	1	0.02079	0.9517
3.7 Hz	0.02079	1	0.01832
16.1 Hz	0.9517	0.01832	1

results served as data for modal analysis using the Enhanced Frequency Domain Decomposition (EFDD) method in ARTeMIS Modal. To utilize ARTeMIS Modal, three inputs are required (see Figure 9):

1. Geometry input,
2. Data preparation,
3. Degree of Freedom (DOF) assignment.

The geometry input was used to visually represent the structural shape simply in accordance with its actual structure. Data preparation involved putting the accelerometer response recordings obtained from the dynamic load test into the program. Then, the DOF assignment involves positioning the accelerometers on the geometry input and connecting them with the accelerometer response data that was prepared before. Once the inputs are completed, all his data was processed to create a singular value of spectral density graph (see Figure 10).

Table 3. Results from Numerical Model using Midas Civil

Mode No	Frequency		Period
	(rad sec^{-1})	(cycle sec^{-1})	(sec)
1	19.242	3.062	0.326
2	21.957	3.494	0.286
3	63.937	10.175	0.098
4	74.570	11.868	0.084
5	78.443	12.484	0.080
6	124.918	19.881	0.050

Using EFDD, modal parameters were extracted. Figure 11 showed graphs of singular value of spectral density with modes at three frequency points. The extracted modal frequencies were 3.09 Hz, 3.745 Hz, and 16.122 Hz. The first and second mode frequencies are close to each other, known as close mode frequency, which can vary depending on the structural aspects such as boundary condition, mass, stiffness, and other dynamics factors. However, since EFDD method only used acceleration data from the dynamic load test, the method is robust enough to determine the modes.

Further analysis using the logarithmic decrement method from EFDD revealed that the damping ratios at each frequency to be 3.431%, 1.68%, and 0.845% respectively (see Table 1). The respective mode shapes were the vertical bending mode, torsional mode, and

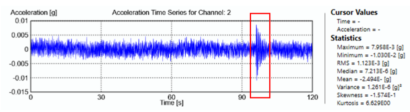

(a) Accelerometer 2

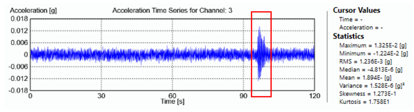

(b) Accelerometer 3

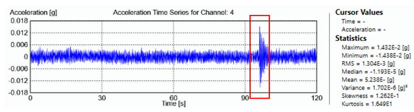

(c) Accelerometer 4

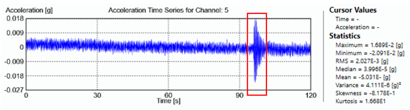

(d) Accelerometer 5

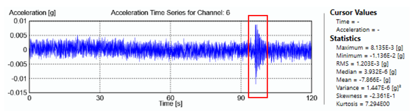

(e) Accelerometer 6

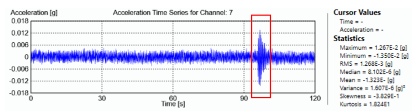

(f) Accelerometer 7

Figure 6 Raw data recorded from accelerometer used in the dynamics load test

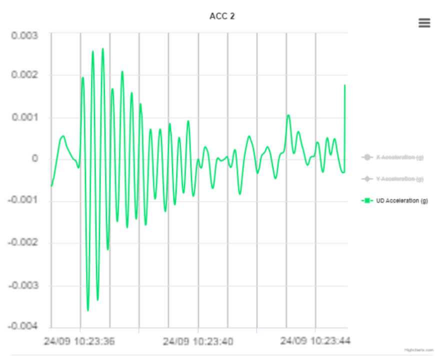

(a) Accelerometer 2

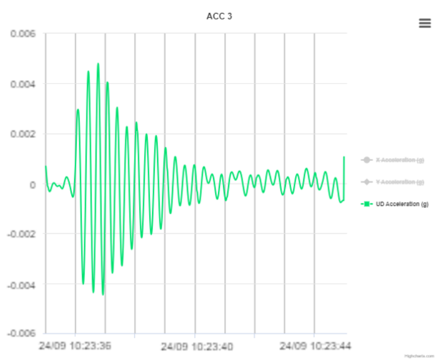

(b) Accelerometer 3

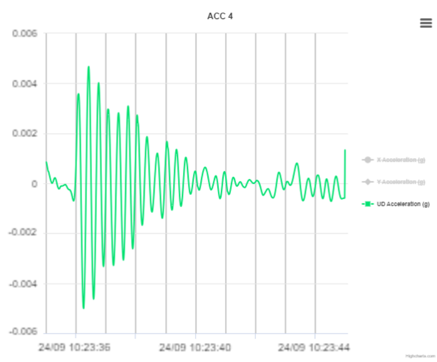

(c) Accelerometer 4

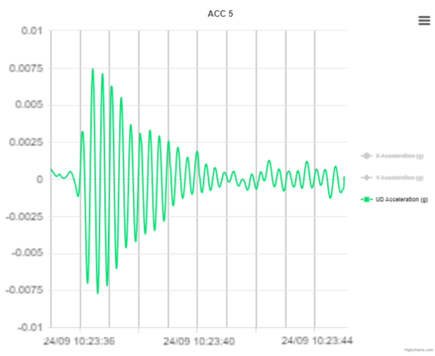

(d) Accelerometer 5

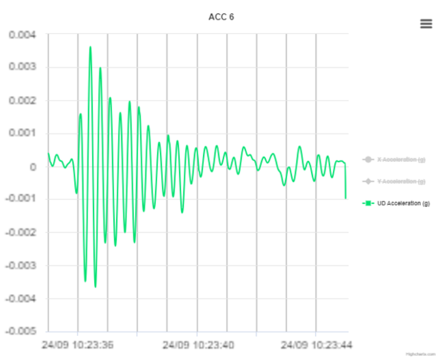

(e) Accelerometer 6

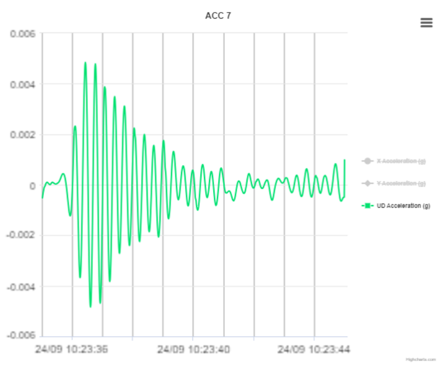

(f) Accelerometer 7

Figure 7 Cut and filtered data recorded from the accelerometer used in the dynamics load test

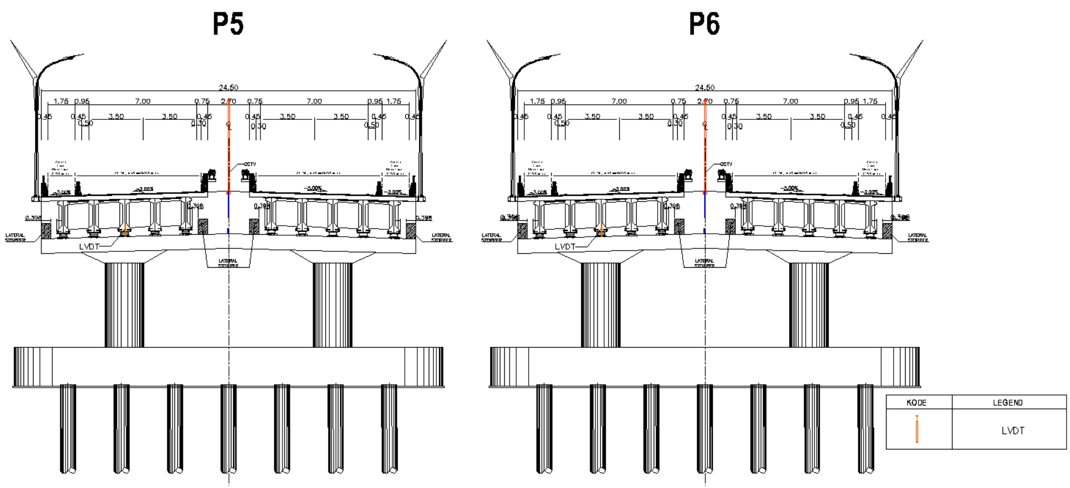

Figure 8 Cross section on P5 Kretek II Bridge

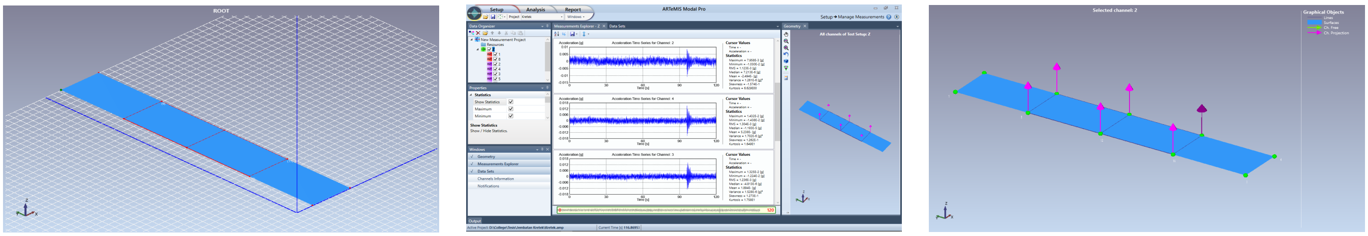

(a) Geometry (b) Data Preparation (c) Assigning DOF

Figure 9 Input data on ARTeMIS Modal

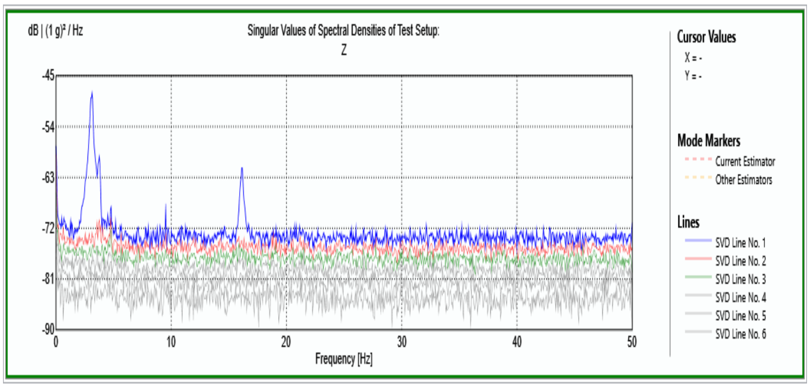

Figure 10 Singular value of spectral density of P5-P6 Kretek II bridge

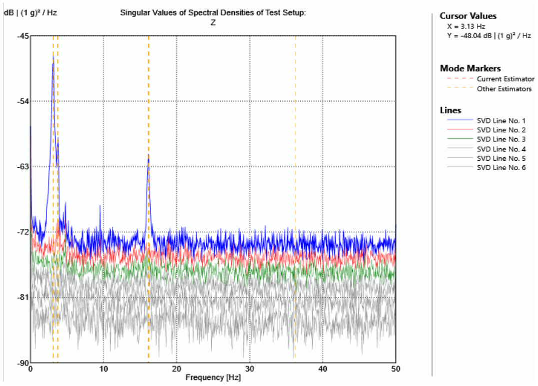

Figure 11 EFDD Result from singular value of spectral density of P5-P6 Kretek II bridge

Table 4. Modal mass participation of the numerical model results

Mode No	TRAN-X		TRAN-Y		TRAN-Z		ROTN-X		ROTN-Y		ROTN-Z	
	MASS (%)	SUM (%)	MASS (%)	SUM (%)	MASS (%)	SUM (%)	MASS (%)	SUM (%)	MASS (%)	SUM (%)	MASS (%)	SUM (%)
1	0.58	0.58	0	0	71.62	71.62	0	0	0.06	0.06	0	0
2	0	0.58	4.69	4.69	0	71.62	67.3	67.3	0	0.06	0	0
3	0	0.58	53.85	58.54	0	71.62	4.84	72.14	0	0.06	0.71	0.71
4	3.65	4.23	0	58.54	0.01	71.64	0	72.14	38.54	38.6	0	0.71
5	0	4.23	11.35	69.89	0	71.64	0.64	72.78	0	38.6	3.62	4.33
6	72.78	77.01	0	69.89	0.02	71.65	0	72.78	1.21	39.81	0	4.33

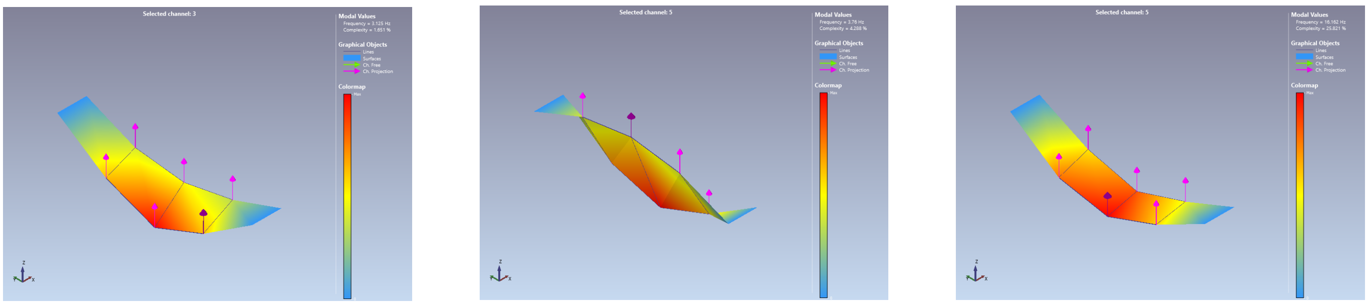

(a) 1^{st} Mode (vertical bending) (b) 2^{nd} mode (torsion) (c) 3^{rd} mode (vertical bending)

Figure 12 Modeshape results from EFDD in ARTeMIS Modal

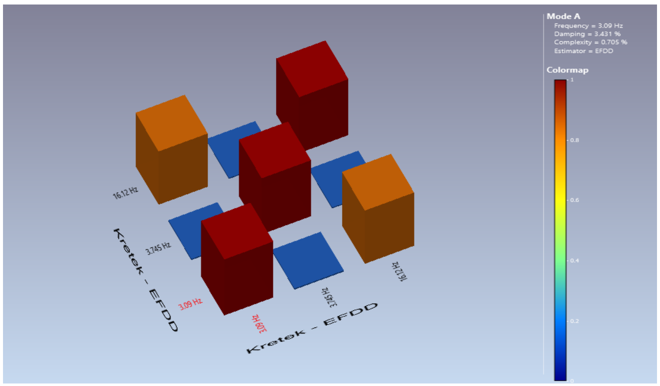

Figure 13 MAC Comparison between each mode from EFDD in ARTeMIS Modal

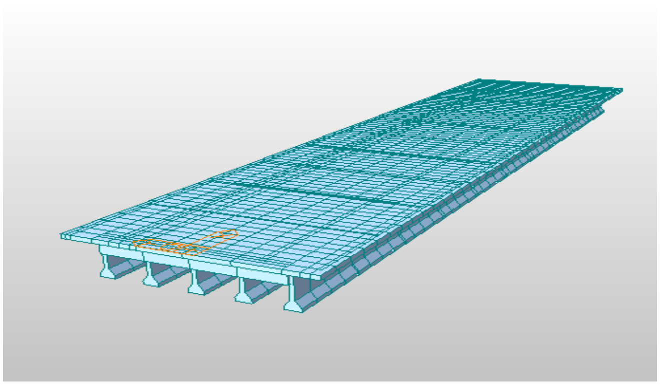

Figure 14 Numerical model of Kretek II bridge

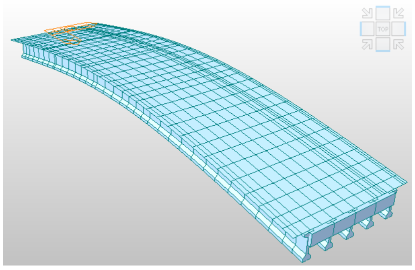

(a) 1^{st} mode

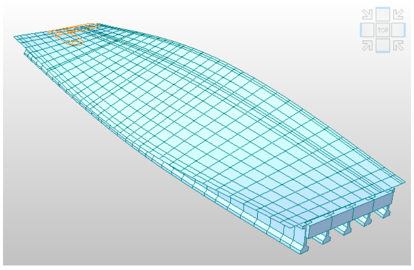

(b) 2^{nd} mode

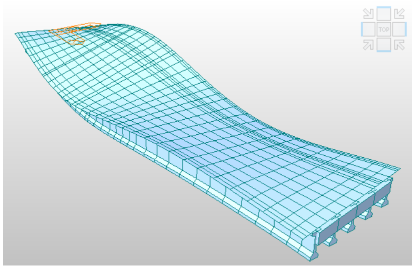

(c) 3^{rd} mode

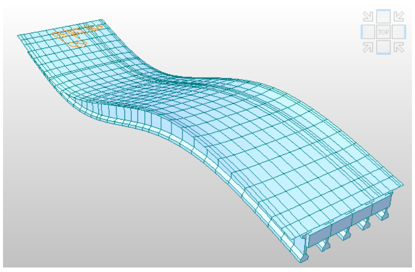

(d) 4^{th} mode

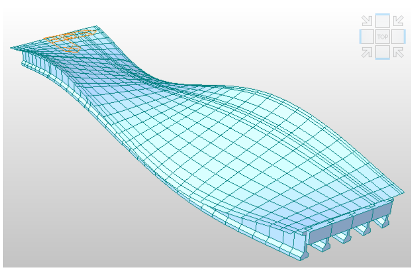

(e) 5^{th} mode

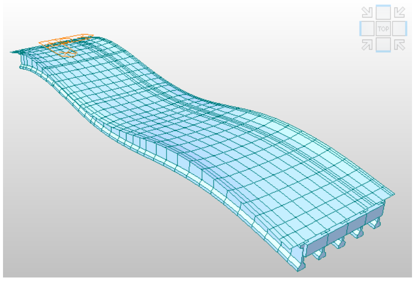

(f) 6^{th} mode

Figure 15 Modeshape results from numerical modell using Midas Civil

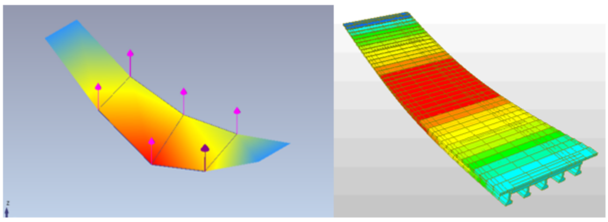

(a) 1^{st} mode comparison

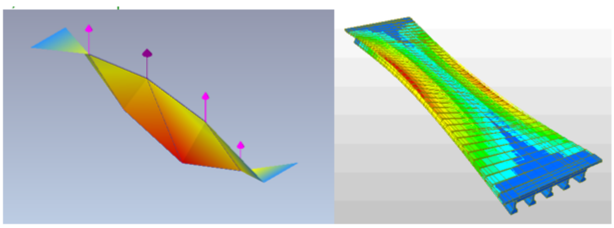

(b) 2^{nd} mode comparison

Figure 16 Side-by-side comparison between 1st mode and 2nd mode using EFDD and Numerical Model

Table 5. Comparison between EFDD results and numerical model results

Mode No	Frequency (Hz)		Error (%)
	Numerical Model	EFDD	
1	3.06	3.09	0.89
2	3.49	3.745	7.17
3	10.175	-	-
4	11.868	-	-
5	12.484	-	-
	-	16.122	-
6	19.881	-	-

another vertical bending mode. From a complexity perspective, the first mode was considered a simple mode shape with low complexity at only 0.71%, while the other two modes were considered complex modes, with percentages of 13.5% and 18.85%, respectively (see Figure 12). Upon careful examination, the first and third mode shapes were the same vertical bending mode. To assess the relationship and similarity between both mode shapes, Modal Assurance Criterion (MAC) was performed.

4.2 Modal Assurance Criterion

In simple terms, the Modal Assurance Criterion (MAC) assessed the similarity between mode shapes results for each mode. A MAC value close to zero indicated significant differences, while a value close to one signified high similarity. Figure 13 and Table 2 summarized MAC values. Results showed MAC values of 0.2 between the first and second modes, 0.18 between the second and third modes, and 0.9517 between the first and third modes. Near-zero MAC values for the first two modes indicated significant differences, while the high value for the first and third modes suggests strong similarity. However, finding two dissimilar wide-range frequencies having identical mode shapes is challenging in theory. This is likely due to the limited number of degrees of freedom (DOF) assigned (accelerometer used) in the dynamic load test, causing the mode shapes to look very similar (Pastor et al., 2012). Nonetheless, such complexity is unnecessary and may hinder calculations.

4.3 Numerical Modeling

To validate the results obtained from the EFDD method, numerical modeling was performed using Midas Civil software. The numerical models were constructed to closely match the actual structure of the Kretek II bridge based on the Detailed Engineering Drawings (DED), ensuring a similar modal analysis to the real-world conditions (see Figure 14). The results indicated modal frequencies for the first six modes as follows: 3.06 Hz, 3.49 Hz, 10.17 Hz, 11.86 Hz, 12.48 Hz, and 19.88 Hz (see Table 3). From this modal analysis, the mode shape for each mode could be determined (see Figure 15).

To objectively analyze the mode shapes in the numerical modeling, it is essential to examine the modal mass participation of each mode (see Table 4). The results indicated that the first mode (3.06 Hz) exhibited significant mass participation in the Z-axis translation, with a total of 71.62%. Similarly, the second mode (3.49 Hz) showed a significant mass participation in the X-axis rotation, with total of 67.3%. These findings confirmed that the mode shapes observed in the Kretek II Bridge correspond to the vertical bending mode for the first mode and the torsional mode for the second mode.

4.4 Comparison between EFDD results and numerical modeling results

The comparison between EFDD and numerical modeling results revealed excellent agreement, with percentage errors in mode frequencies for the first and second modes at 0.89% and 7.17%, respectively (see Table 5). These insignificant discrepancies suggest strong alignment between EFDD and numerical modeling outcomes. Upon visual inspection, both methods sowed correspondence for the first and second mode, with the first exxhibiting a vertical bending mode, while the second torsional mode (see Figure 16). However, subsequent modes did not exhibit similarities, possibly due to EFDD relying solely on Z-axis acceleration data, resulting in the identification of only certain modes. This discrepancy led to larger errors in the comparison with numerical modelling results.

5 CONCLUSION

The natural frequencies extracted from the acceleration data using the EFDD were 3.09 Hz, 3.49 Hz, and 16.122 Hz, corresponding to different mode types: vertical bending mode, torsional mode, and another vertical bending mode, respectively. Although the first and the third modes both exhibited a vertical bending mode with a 0.95 MAC value, it's likely that they had different shapes. This could be attributed to the limited degrees of freedom (DOF) assigned (accelerometer sensors placed) during the dynamic load test, which may make them appear similar.

The natural frequencies obtained from numerical modeling were 3.06 Hz, 3.49 Hz, 10.17 Hz, 11.86 Hz, 12.48 Hz, dan 19.88 Hz. The first two modes corresponded to the vertical bending mode and torsional mode, confirmed by examining the modal mass participation. Both EFDD and numerical modeling results were in agreement, with errors between the first two modes were 0.89% and 7.17%, indicating very good agreement. Additionally, the mode shapes of the first two modes were consistent when compared side by side between EFDD and numerical modeling results.

DISCLAIMER

The authors declare no conflict of interest.

REFERENCES

Brincker, R. and Ventura, C. E. (2015), *Introduction to Operational Modal Analysis*, Wiley.

Brincker, R., Ventura, C. E. and Andersen, P. (2001), Damping estimation by frequency domain decomposition, *in* 'Proceedings of IMAC 19: A Conference on Structural Dynamics', Hyatt Orlando, Kissimmee, Florida, pp. 698–703.

Brincker, R. and Zhang, L. (2009), Frequency domain decomposition revisited, *in* 'Proceedings of the 3rd International Operational Modal Analysis Conference - IOMAC', p. 615.

Brincker, R., Zhang, L. and Andersen, P. (2000*a*), Modal identification from ambient responses using frequency domain decomposition, *in* 'Proceedings of the International Modal Analysis Conference (IMAC)', Vol. 18, San Antonio, Texas, USA, pp. 625–630.

Brincker, R., Zhang, L. and Andersen, P. (2000*b*), Modal identification of output-only systems using frequency domain decomposition, *in* 'Proceedings of the European COST F3 Conference on System Identification & Structural Health Monitoring', Universidad Politécnica de Madrid, Spain, pp. 273–282.

Brincker, R., Zhang, L. and Andersen, P. (2000*c*), Output-only modal analysis by frequency domain decomposition, *in* 'Proceedings of ISMA25: 2000 International Conference on Noise and Vibration Engineering', Katholieke Universiteit, Leuven, pp. 717–723.

El-Borgi, S., Smaoui, H., Cherif, F., Bahlous, S. and Ghrairi, A. (2004), 'Modal identification and finite element model updating of a reinforced concrete bridge', *Emirates Journal for Engineering Research* **9**.

Ghalishooyan, M., Shooshtari, A. and Abdelghani, M. (2019), 'Output-only modal identification by in-operation modal appropriation for use with enhanced frequency domain decomposition method', *Journal of Mechanical Science and Technology* **33**, 3055–3067.
URL: *https://doi.org/10.1007/s12206-018-0906-1*

Ma, J. and Luan, W. (2020), Modal identification of a building structure by frequency domain decomposition, *in* 'IOP Conference Series: Materials Science and Engineering', Vol. 794, Institute of Physics Publishing.
URL: *https://doi.org/10.1088/1757-899X/794/1/012048*

Mao, Q., Mazzotti, M., DeVitis, J., Braley, J., Young, C., Sjoblom, K., Aktan, E., Moon, F. and Bartoli, I. (2019), 'Structural condition assessment of a bridge pier: A case study using experimental modal analysis and finite element model updating', *Structural Control and Health Monitoring* **26**.
URL: *https://doi.org/10.1002/stc.2273*

Morris, A. S. and Langari, R. (2012), *Measurement and Instrumentation Theory and Application*, Vol. 7 of *Syria Studies*.

Orlowitz, E. and Brandt, A. (2017), 'Comparison of experimental and operational modal analysis on a laboratory test plate', *Measurement: Journal of the International Measurement Confederation* **102**, 121–130.
URL: *https://doi.org/10.1016/j.measurement.2017.02.001*

Pastor, M., Binda, M. and Harčarik, T. (2012), Modal assurance criterion, *in* 'Procedia Engineering', Vol. 48, Elsevier Ltd, pp. 543–548.
URL: *https://doi.org/10.1016/j.proeng.2012.09.551*

Salawu, O. S. (1997), 'Detection through changes a review', *Engineering Structures* **19**, 718–723.

Schwarz, B. J. and Richardson, M. H. (1999), 'Experimental modal analysis'.

Sevim, B., Bayraktar, A., Altunişik, A. C., Adanur, S. and Akköse, M. (2010), 'Modal parameter identification of a prototype arch dam using enhanced frequency domain decomposition and stochastic subspace identification techniques'.

Silva, M. S. and Neves, F. A. (2020), 'Modal identification of bridge 44 of the carajás railroad and numerical modeling using the finite element method', *Revista IBRACON de Estruturas e Materiais* **13**, 39–68.
URL: *https://doi.org/10.1590/s1983-41952020000100005*

Zair, D. B. A. H., Bin Abu Hasan, M. D., Ahmad, Z. A. B., Leong, M. S. and Hee, L. M. (2020), 'A study of the parameters that affect the quality of the estimated modal parameters in automated enhanced frequency domain decomposition algorithm', *Pertanika J. Sci. & Technol* **28**, 797–828.